

OMA2022-80636

## A REDUCED ORDER PARAMETERIZATION OF RANDOM WAVE FIELDS WITH DETERMINISTIC WAVE GROUPS

Tianning Tang<sup>1</sup> and Thomas A. A. Adcock<sup>1</sup>

<sup>1</sup>Department of Engineering Science, University of Oxford, Oxford, UK

### ABSTRACT

*Under a linear model of gravity wave evolution the expected shape of large events is given by Quasi-determinism theory. However, nonlinear physics modifies the averaged shape of the largest events. In this study, we examine these nonlinear modifications to the averaged shape of the largest events for directionally spread random wave fields. We first compare these nonlinear changes from the extreme events in random wave fields with the nonlinear changes during the evolution of deterministic wave groups. We then explore whether it is possible to predict these nonlinear changes observed in random wave fields with only nonlinear wave group simulations. We applied a modified version of the wave group detection algorithm in [1, 2] to isolate the individual wave groups from random wave fields. We perform the nonlinear wave group simulations with the initial conditions matching these isolated individual wave groups extracted from linear random wave field. The nonlinear evolution of these isolated wave groups can predict the envelope contraction of averaged shape of extreme events in random wave fields quantitatively over a wide range of local steepness under current conditions. This suggests some statistical connections between the nonlinear evolution of deterministic wave groups and the evolution of the largest waves in the random wave fields.*

### 1 Introduction

The term “freak waves” or “rogue waves” usually refers to extremely large but rarely occurring waves in the open ocean. There is a lot of interest in the physics and engineering communities about the most probable shape of these freak waves as the shape is related to the wave dynamics and the wave-induced

forces in ocean engineering practice [3–5]. For real water waves in the open ocean, the amplitude and the phase component of these wind generated waves are randomly distributed, which leads to each individual extreme having a different shape. In linear theory, Quasi-determinism theory applies, suggesting the expected shape of extreme waves is given by NewWave, which says that the expected shape of an extreme event tends to the autocorrelation function [6–8] (see also higher-order models in [9]).

When investigating extreme events, deterministic wave groups have the advantage in saving computational cost and experimental time, as large events rarely happen in random time series. More importantly, because the NewWave group shape is also interconnected with the averaged shape of the largest events in the random time series (according to linear theory), various studies focus on the change in the shape during the nonlinear evolution of groups which under linear evolution would have formed a NewWave group. Numerical [10] and analytical [11] work predicts that nonlinear physics would modify the shape of these NewWave groups including the contraction of the wave group in the mean wave direction, expansion in the lateral direction, and horizontal asymmetry with the largest wave moving to front of the packet. Although these predictions are based purely on the nonlinear evolution of deterministic NewWave groups, similar nonlinear changes can also be observed for the largest events in random time series on average with numerical simulations and experiments (see further details in [12–16]). Some of these changes have been observed in real water waves in the open ocean [17, 18].

The nonlinear changes observed in the shape of large events in both deterministic wave groups and random wave fields seems to suggest that the evolution of water waves in both situa-

tions are modified by similar nonlinear processes. Apart from the Quasi-determinism theory, which connects the deterministic wave groups and the random sea on a linear basis, a more sophisticated data-centric method has been proposed for isolating wave groups from random time series [2, 19]. A modified version from [1,20] has also been used for predicting the space-time wave statistics. The accurate statistical prediction based on the wave group detection method indicates that these carefully designed wave groups can provide accurate prediction of the nonlinear amplification in random time series.

In this study, we apply the modified wave group detection method proposed in [1] for averaged shape predictions. Previously it has only been used for predicting crest statistics. We will compare the performance when predicting the nonlinear changes in random time series with the wave group detection method, as well as the NewWave based method. Both of the methods use the nonlinear simulations of deterministic wave groups for estimating the nonlinear changes in nonlinear random time series. In the former method, the largest wave group profiles from linear random time series are extracted and used in the initial conditions of deterministic wave groups. We let these carefully designed wave groups evolve nonlinearly and the averaged shape of these wave groups at nonlinear focus is used to predict the changes in nonlinear random time series. For the latter method, the NewWave groups are scaled to the top 100 largest events, which is then used as the initial conditions in the nonlinear simulations. The accuracy of both prediction methods is evaluated with three different sampling domain sizes.

We structure this paper as follows. We first provide a brief introduction of the wave group detection algorithm used in this study in Section 2. We then provide all the numerical details in Section 3.1 and present results in Section 4.

## 2 Wave group detection from random wave fields

In this study, we aim at connecting the nonlinear changes observed during the evolution of deterministic waves to make computationally efficient predictions for random time series. This connection process starts with isolating all the largest wave groups within random linear simulations. Because of the inherent randomness of the wave field, it is rather difficult to isolate and extract wave groups directly. Instead, we followed the wave group detection method proposed in [1] and use a superposition of Gaussian elementary wave groups to match the spatial profile of a linear wave field as:

$$G(x,y) = \sum_{n=1}^N g_n(x,y), \quad (1)$$

where  $G(x,y)$  is the superpositioned wave field, and  $N$  is the number of wave groups with a Gaussian profile  $g_n(x,y)$  as:

$$g_n(x,y) = A_n \exp \left[ -\frac{(x-x_n^c)^2}{(L_n^x)^2} \right] \exp \left[ -\frac{(y-y_n^c)^2}{(L_n^y)^2} \right], \quad (2)$$

where  $A_n$  is the envelope height of  $n^{th}$  wave group with the wave group centre at  $(x_n^c, y_n^c)$  and the  $L_n^x$  and  $L_n^y$  are the two length scale parameters measuring the width of the group in the longitudinal direction  $x$  and in the transverse direction  $y$  respectively.

We summarise the wave group detection method below given full details are presented elsewhere [1]. We first identify the wave group centres by finding the local maximum point of the random wave field. We then run an optimisation algorithm to determine the best-fits for the length scale parameters for all the wave groups. This fictitious time scale marched optimisation algorithm starts with the initial conditions defined to match the second order derivatives at the envelope peak and will terminate when the desired level of accuracy is achieved.

This wave group detection method effectively decomposes the entire random wave fields into individual Gaussian wave groups and we present a typical wave group detection results in Figure 1. The wave group detection method proposed can capture most of the envelope shapes in a random wave field and we will examine the accuracy of this wave group detection algorithm later in the study.

## 3 Numerical Details

In this study, we investigate the averaged shape of the largest events in a two-dimensional water wave system. We will also examine the performance of the wave group detection method and the NewWave theory based method in predicting the shape changes of the largest events during the nonlinear evolution. A total of four different sets of simulations are performed in this study which are detailed in Table 1. All the nonlinear simulations in this study are performed with the Modified Nonlinear Schrodinger Equation (MNLS) [21] (see details in Section 3.1).

We have examined three cases of interest and these cases cover an Eulerian point measurement, averaged shape from an intermediate sized area, and the averaged shape from a large area.

**TABLE 1.** Types of simulations performed in this study.  $T_p$  is the peak wave period.

Name	Type of simulation	Linearity	No. of simulations	Length
Linear Random Sea	Random waves	Linear	4000 Realisations	40 $T_p$
Nonlinear Random Sea	Random waves	Nonlinear	4000 Realisations	40 $T_p$
Decomposed Wave Groups	Gaussian Wave Group	Nonlinear	27000 Cases	30 $T_p$
NewWave Groups	NewWave Group	Nonlinear	100 Cases	30 $T_p$

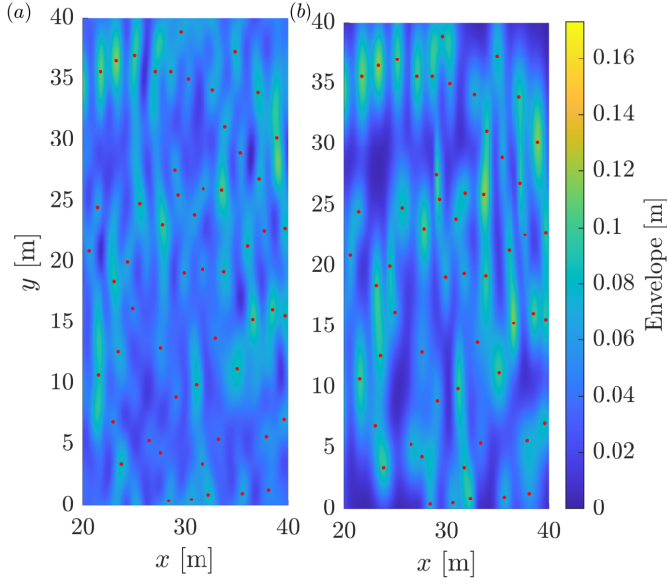


**FIGURE 1.** Wave envelope field for (a): a sample low-pass filtered envelope field from random linear simulations and (b): superpositioned wave envelope field  $G(x,y)$  reconstructed with decomposed elementary Gaussian wave groups  $g_n(x,y)$ . Red dots represents the position of detected wave group centre with peak detection algorithm. The wave field is generated with a initial Gaussian spectrum with the spectral bandwidth in  $x$  and  $y$  direction to be  $\sigma_x = \sigma_y = 0.1$ . The wave steepness of this wave field is  $H_s k_p = 0.25$ .

The scale of the area relative to the wavelengths are presented in Table 2.

### 3.1 MNLS equation

In this study, we calculate numerical solutions of the MNLS from [21] (please see [22, 23] for a detailed comparison of the performance of this numerical scheme).

The MNLS is a nonlinear model for the evolution of the complex envelope,  $u$ :

**TABLE 2.** Summary of simulations in this study, where  $H_s$  is the significant wave height,  $k_p$  is the peak wavenumber,  $T_p$  is the peak period,  $\sigma_x$  and  $\sigma_y$  are the spectral bandwidth in  $x$  and  $y$  direction and  $\lambda_p$  peak wavelength.

Case	$H_s k_p$	$T_p$ [s]	$\sigma_x$	$\sigma_y$	Quantity of interest	Sampling domain ( $\mathcal{S}$ )
1	0.25	2	0.1	0.1	$ u /H_s$	Centre point
2	0.25	2	0.1	0.1	$\max_{x,y \in \mathcal{S}}  u(x,y) /H_s$	$x \in [0, 3\lambda_p], y \in [0, 3\lambda_p]$
3	0.25	2	0.1	0.1	$\max_{x,y \in \mathcal{S}}  u(x,y) /H_s$	$x \in [0, 10\lambda_p], y \in [0, 10\lambda_p]$

$$\frac{\partial u}{\partial t} + L(\partial_x, \partial_y)u + \frac{i\omega_0 k_p^2}{2}|u|^2 u + \frac{3\omega_0 k_p}{2}|u|^2 \frac{\partial u}{\partial x} + \frac{\omega_0 k_p}{4} u^2 \frac{\partial u^*}{\partial x} + ik_p \frac{\partial \phi}{\partial z} \Big|_{z=0} u = 0, \quad (3)$$

where  $\omega_0$  is the peak angular frequency,  $k_p$  is the peak wave number,  $*$  represents the complex conjugate,  $z$  is the vertical coordinate, and the linear operator  $L(\partial_x, \partial_y)$  is given as:

$$L(\partial_x, \partial_y) = i \left\{ \left[ (1 - i\partial_x)^2 - \partial_y^2 \right]^{1/4} - 1 \right\}, \quad (4)$$

and the return current potential  $\phi$  is calculated with

$$\frac{\partial \phi}{\partial z} \Big|_{z=0} = \frac{\omega_0}{2} \frac{\partial |u|^2}{\partial x}, \quad (5)$$

and the potential followed Laplace's equation within the fluid domain, hence  $\nabla^2 \phi = 0$ , and  $\phi$  tends to zero in the limit as  $z \rightarrow -\infty$ . the surface of free waves can be obtained from the complex envelope  $u$  using the following:

$$\eta = \text{Real}(u \exp(i(k_0 x - \omega_0 t))). \quad (6)$$

We used a fixed time step of 0.04 seconds (50 steps per peak period) for all the nonlinear simulations with MNLS.

### 3.2 Random wave field

In this study, we focus on the averaged shape of the largest events from a random wave field. Hence, the linear and nonlinear random wave fields are simulated as the baseline for examining the overall performance of wave group detection method and the NewWave theory based method. Following [24], we setup a numerical domain with periodic boundary conditions in both directions, with the number of grid points in  $x$  and  $y$  direction to be  $N_x = N_y = 128$ . We consider waves with a peak period of  $T_p = 2$  seconds, which corresponds to a peak wavelength of  $\lambda_p = 2\pi$  meters for deep water waves. The numerical domain has 10 wavelengths in  $x$  and 20 wavelengths in  $y$ , and the discretisation of the wave vector plane are  $\Delta K_x = 1/(10\lambda_p)$  and  $\Delta K_y = 1/(20\lambda_p)$ . This gives a physical length in  $x$   $D_x = 2\pi/\Delta K_x$  and  $D_y = 2\pi/\Delta K_y$  in  $y$  direction with individual grid points:  $x_j = D_x j/N_x, j = 0, 1, \dots, N_x - 1$  and  $y_l = D_y l/N_y, l = 0, 1, \dots, N_y - 1$ .

We start our simulation with a initial Gaussian envelope

spectrum as:

$$\psi_{mn} = \frac{\varepsilon}{\sqrt{2\pi\sigma_x\sigma_y}} \exp \left[ -\frac{(m\Delta K_x)^2}{4\sigma_x^2} - \frac{(n\Delta K_y)^2}{4\sigma_y^2} \right], \quad (7)$$

where the  $\sigma_x = \sigma_y = 0.1$  is the spectral bandwidth in  $x$  and  $y$  direction.  $\varepsilon$  is the wave steepness scaling factor, which controls the significant wave height. In this study, we tune the  $\varepsilon$  to match the target wave steepness of  $H_s k_p = 0.25$  for both linear and nonlinear random simulations, where  $H_s$  is the significant wave height of the random wave field and  $k_p$  is the peak wavenumber. The Fourier components  $\hat{B}_{mn}$  can be obtained by adding a random phase to the wave spectrum as:

$$\hat{B}_{mn} = \sqrt{\Delta K_x \Delta K_y} \psi_{mn} \exp i\theta_{mn}, \quad (8)$$

where  $i$  is the imaginary unit, and  $\theta_{mn}$  is the random phase, which uniformly distributes within the interval  $[0, 2\pi]$ .

It is slightly more complicated to calculate the averaged shape of the largest events especially when areal measurements are considered. In this study, we focus on the wave group, which causes the largest surface elevation within the sampling domain ( $\mathcal{S}$ ) over the entire duration of the simulation. The detected wave group is centred in space and collected for all the linear and nonlinear random simulations. In this study, a total of 4,000 largest envelope profiles are collected and averaged to obtain the final results.

### 3.3 Decomposed wave group simulations

In this study, we explore whether we can make accurate predictions on the average shape of the largest events based on the wave group detection method introduced in Section 2. To achieve this, we follow a similar approach in the previous studies [10, 25–27] and use the evolution of focused wave groups as a convenient proxy for including the nonlinear effects during the wave evolution. To focus on the largest events, we only considered all the wave groups with a nonlinear amplification ( $A_{max}/A$ ) greater than 1.05, where  $A_{max}$  is the maximum amplitude of a wave group under nonlinear evolution. We obtain the nonlinear evolution of these wave groups with the numerical simulation of a wave group, which will form a perfect linear focused wave group after 15 peak wave periods. Since the nonlinear physics also modifies the focus time, additional 15 peak wave periods (30 in total) are simulated to capture the entire nonlinear focusing and de-focusing processes.

We obtain the parameters of extreme wave groups from random linear wave fields with the wave group detection method proposed in Section 2. These collected extreme wave group parameters are then used to define the envelope profile of deter-

ministic wave groups at linear focus. Because it is too computationally intensive to simulate all detected extreme wave profiles, we binned these parameters with 30 uniformly distributed bins in both  $L_x$  and  $L_y$ , and also 31 uniformly distributed bins for  $A$ . These bins cover a wide parameter space as:

$$L_x k_p \in [1, 14], \quad L_y k_p \in [4, 40] \quad \text{and} \quad A k_p \in [0.07, 0.38]. \quad (9)$$

A total of 27900 cases of wave groups are simulated to cover all the combinations of wave group parameters within the parameter space. During the averaging process, a weighted function is introduced to prioritise the most common combination of wave group parameters found during the wave group detection process, and the weight function can be simply approximated as the joint distribution of three wave group parameters ( $A$ ,  $L_x$  and  $L_y$ ).

For the wave group simulations with wave group detection method we use a computational domain with 256 points in  $x$  direction and 128 points in  $y$  direction. Periodic boundary conditions are employed in both horizontal directions. Due to the wide range of wave group sizes considered in this study, the physical domain size is adjusted from 4 wavelengths to 40 wavelengths in  $x$  direction and from 4 wavelengths to 20 wavelengths in  $y$  direction. A fixed time steps of 0.04 seconds are used (50 steps per period) for wave group simulations.

### 3.4 NewWave group simulations

Under a linear model of wave evolution, the theory of Quasi-determinism predicts the averaged shape of extreme waves [6, 8, 28]. The most probable shape of an extreme crest can be calculated with the scaled auto-correlation function [7]. In the spatial domain, the expected shape of wave group with an extreme crest  $\bar{\eta} = \eta_{max}$  can be obtained as:

$$\begin{aligned} \bar{\eta}(x, y, t) = & \eta_{max}/m_0 \int_0^\infty \int_0^{2\pi} S(\omega, \theta) \\ & \times \cos(k_0 x \sin \theta + k_0 y \cos \theta - \omega T) \\ & \times d\theta d\omega, \end{aligned} \quad (10)$$

where  $S(\omega, \theta)$  is the directional power spectral density function,  $k_0$  is the peak wave number, and  $m_0$  is the zeroth moment of the wave spectrum.

In this study, we scaled the NewWave groups to the top 100 largest wave groups isolated using the wave group detection method. We follow the procedure for decomposed wave group simulations and run the nonlinear simulation from  $-15T_p$  to  $15T_p$  after the linear focus. The wave envelope profile at linear focus is now matched for the scaled NewWave profile presented in Equation 10.

For NewWave group simulations, we use a computational domain with 512 points in  $x$  direction and 256 points in  $y$  direction with periodic boundary conditions employed in both horizontal directions. The physical domain size is fixed at 20 wavelengths in both  $x$  and  $y$  directions. A fixed time steps of 0.04 seconds are used (50 steps per period) for wave group simulations.

## 4 Results

In this study, we investigate the nonlinear changes to the average shape of the largest events in random wave fields with deterministic wave groups. We examine two methods for this prediction. The first prediction method involves isolating individual wave groups from the linear random field using the wave group detection algorithm. A set of carefully designed wave groups are simulated with nonlinear evolution to predict the nonlinear changes in the random time series on average (see Section 3.3 for details). The second method uses the NewWave group shape based initial conditions for nonlinear simulations of deterministic wave groups. The NewWave group shape is scaled to the top 100 largest waves found in the linear random field. The nonlinear evolution of these scaled NewWave groups are averaged to predict the nonlinear changes in the random time series (see Section 3.4 for details). The performance of these methods is then compared to the averaged shape of the largest events in the nonlinear random wave simulations in Section 4.4.

### 4.1 Averaged shape of largest events from random wave fields

We first present the target averaged shape of the largest events in the random wave simulations for Case 2 and Case 3 in Figure 2. In Figure 2 ( $a, b$ ), we show the normalised averaged envelope profile from linear random wave field. The overall shape of these averaged envelopes is consistent with the predictions from Quasi-determinism theory. The average profile is close to being perfectly symmetric in both directions, and the shape seems to be well captured by a Gaussian wave group shape (see detailed comparisons in Section 4.4). Additionally, the wave groups are elongated in the lateral direction when the sampling domain becomes larger. This agrees well with previous studies [1], as they observe the length scale in  $y$  direction almost doubled when a larger area is sampled. We note that this ‘linear’ expansion in the lateral direction is very different from the nonlinear expansion of the wave group mentioned in [11, 12, 29], where the latter depends on the nonlinearity instead of the sampling area.

In Figure 2 ( $c, d$ ), we present the averaged shape of largest events in the nonlinear random wave simulations with the same sea states as the linear simulations. When compared to linear simulations, nonlinear physics affects the shape of these largest

events. The wave group tends to be more compact in the mean wave direction and the peak of the wave group tends to move to the front of the wave group. These findings agrees well with the previous studies with both numerical simulations [12], unidirectional wave experiments [13], and field observations [18].

We note that in this study, we extract the averaged shape of these largest wave groups with the surface elevation series instead of the envelope using Equation 6. We stack these surface elevation profiles by centring the largest crests and then calculate back to the envelope profile using the Hilbert transformation after the averaging process. There would be minor differences if the average process is performed directly on the envelope, but the averaged envelope tends to a non-zero value far from the centre. As we are primarily interested in the change close to the peak, the general conclusion should hold either way. It is still better to average on the surface elevation profiles as the averaged surface elevation profiles tend to zero far away from the peak and gives the cleaner results shown in Figure 2.

### 4.2 Evolution of decomposed Gaussian wave groups

In this section, we approximate the linear random wave fields with Gaussian wave profiles and perform nonlinear simulations of these isolated deterministic wave groups. We investigate whether similar nonlinear changes observed during random wave simulations can also be predicted with these deterministic wave groups.

We present the averaged shape of the detected Gaussian wave group profile in Figure 3 ( $a, b$ ) for both Case 2 and Case 3. The averaged profile at focus during the nonlinear simulation of these detected wave groups is shown in Figure 3 ( $c, d$ ). Overall, we observe very similar nonlinear changes on the envelope profile to those found in nonlinear random wave simulations. The wave group becomes more compact in the mean wave direction, and the envelope peak moves to the front of the wave group. Detailed comparison of the linear and nonlinear averaged profile will be shown in Section 4.4.

### 4.3 Evolution of NewWave groups

Instead of using the data driven wave group detection algorithm, the averaged profile of the largest waves from linear random time series from an Eulerian point measurement can directly be obtained with Quasi-determinism theory (also referred to as the NewWave group). Hence, it is also possible to predict the nonlinear changes in the random wave fields with nonlinear NewWave group simulations. Unfortunately, to the author’s knowledge, the current Quasi-determinism theory seems only to focus on point measurements. This certainly affects the performance of NewWave based method for the largest wave profiles measured over an area (i.e. Case 2 and 3). Hence, in this study, we also investigate the averaged shape of the largest events measured from the centre point of the numerical domain.

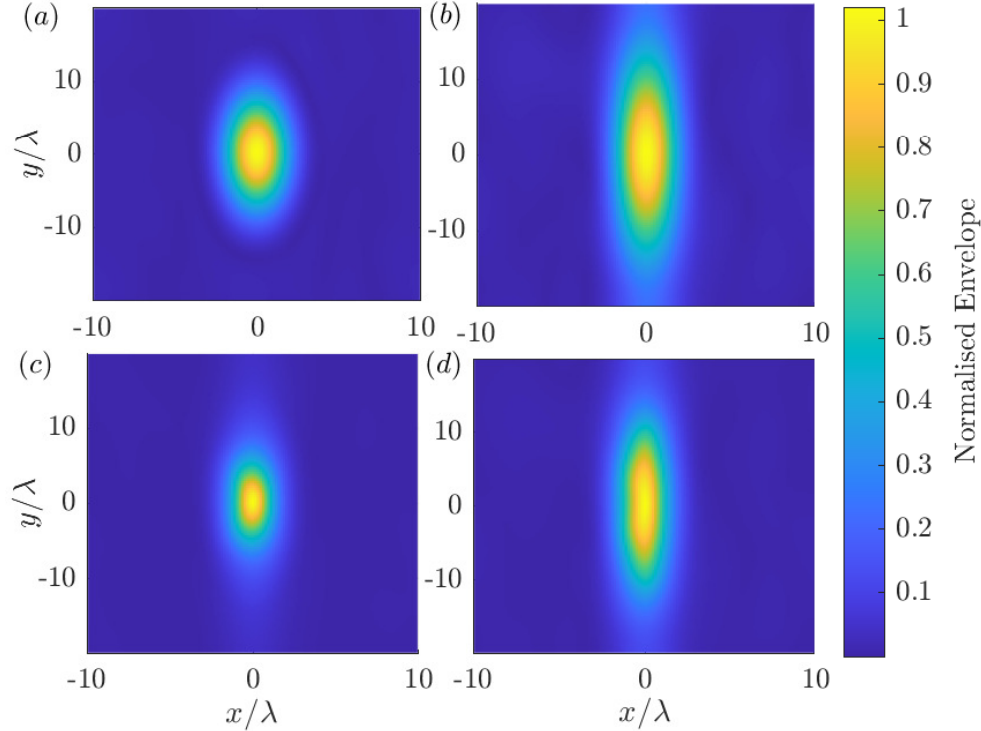


**FIGURE 2.** Averaged shape of Top 3 largest events from (a,b) linear simulation of random wave fields, (c,d) nonlinear random simulations. Figure (a,c) present results for the Case 2 in Table 2 and (b,d) present results for the Case 3 Table 2. Envelope profile are normalised and centred by the maximum value at the envelope peak.

We present the NewWave profile calculated from Equation 10 in Figure 4 (a). The averaged profile of nonlinear NewWave group simulations are shown in Figure 4 (a). Figure 4 (b) and (c) represent the average of profile at nonlinear focus for point measurements and areal measurements respectively. We can still observe all the nonlinear changes from the random time series with NewWave group simulations. However, when this NewWave based method is applied to the areal measurements (i.e. in the Figure 4 (c)), the nonlinear changes are quite dramatic. This could be because of the limitation of Quasi-determinism theory itself and we will present a quantitative comparison in Section 4.4.

#### 4.4 Performance comparison

We first examine the performance of the wave group detection algorithm as well as the Quasi-determinism theory under a purely linear model. Hence, we present the averaged profile of the largest groups from linear random simulation as the ‘ground truth’. Because the Quasi-determinism theory can only be applied to point measurements, only results in Case 1 are considered here. The predicted envelope profile in the mean wave direction from both methods are presented in Figure 5.

As we are primarily interested in the shape of the envelope, not the maximum envelope value, we scaled both envelope profiles to the averaged envelope peak from random wave fields. This is also because the Quasi-determinism theory already scales the NewWave group profile to the maximum surface elevation during the calculation (see Equation 10), it is almost guaranteed to match the peak value between NewWave group profiles and the averaged shape from linear random time series.

From Figure 5, both of the methods capture the averaged shape of the largest events on a linear basis quite well. Some discrepancy can be observed far away from the envelope peak, which is presumably because only a finite number of largest events from random wave fields are considered. This leads to the envelope amplitude being far away from the envelope having a non-zero value. However, for the envelope close to the peak, which is also the profile we are primarily interested in, the NewWave group profile can provide accurate predictions. It also confirms that, on average, the wave group detection algorithm in Section 2 can accurately approximate the largest events from random wave fields with Gaussian shaped envelopes.

We now consider the performance of both methods when predicting the averaged shape of the largest events over an area.

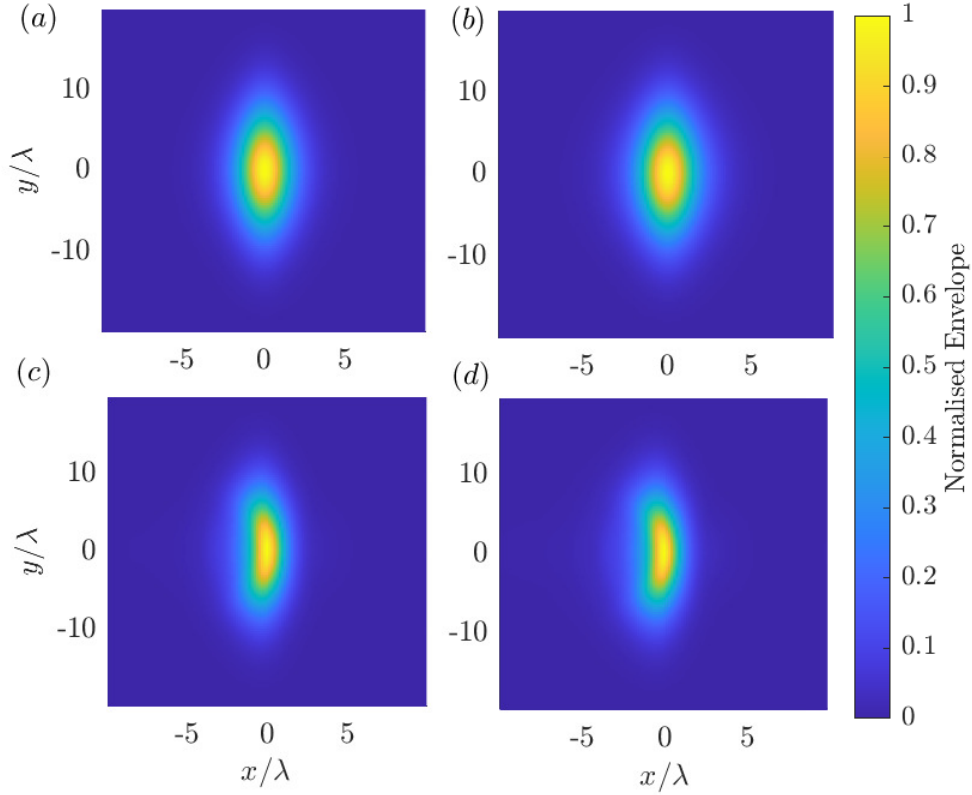


**FIGURE 3.** Averaged shape of decomposed Gaussian wave groups based on the wave group detection method presented in Section 2 for (a,b) averaged decomposed linear wave group profile, (c,d) averaged wave group profile at nonlinear focus. Figure (a,c) present results for the Case 2 in Table 2 and (b,d) present results for the Case 3 Table 2. Envelope profile are normalised and centred by the maximum value at the envelope peak.

In Figure 6 (a), we focus on the linear simulation results and regard the averaged profile from linear random wave fields as the target case for comparison. Overall, the NewWave profile matches the linear averaged shape well and only under predicts the width of the envelope slightly far away from the envelope peak. As it is essentially the same NewWave profile but just with different scaling coefficients for the point measurement in Figure 5. It seems that there are only small increases in the envelope width when the sampling domain enlarges. This agrees well with the previous study [1], where the length scale in  $x$  only changes a little if a larger area is sampled. The wave group detection method overestimates the envelope peak value slightly but can still predict the overall shape accurately. This overestimation is primarily because the wave group detection method essentially averages across a different set of wave groups. As opposed to the largest wave group in each random simulation, the wave group detection method collects all the wave groups within the sampling domain and with a nonlinear amplification factor of 1.05. It is certainly a better categorization for ‘nonlinear’ waves but it is only achievable with the wave group detection method.

In Figure 6 b, we now consider the prediction for the nonlin-

ear changes of the averaged shape of largest events from nonlinear random wave fields. In general, both the NewWave group based method and the wave group detect method show similar nonlinear changes as those observed from the random wave field. However, it seems that directly scaling the NewWave group shape to the top 100 largest crests would result in significant over-prediction in the nonlinear amplification as well as these nonlinear changes. We note that this is a rather simplified prediction process for the NewWave group as there is no suitable formula for areal measurements and the final results also depend on the number of averaged profiles (i.e. top 100 versus top 1000). For the wave group detection method, however, because all the nonlinear simulations are based on isolated wave groups in linear random wave fields, the method can easily accommodate the changes in the sampling domain. This results in accurate predictions in the nonlinear amplification at the envelope peak as well as the nonlinear shape changes.

Finally, we further investigate the applicable range of such predictions with the wave group detection method. To achieve this, we categorised the collected nonlinear wave group profile based on the local wave steepness around the peak ( $A_{nonlinear}k_p$ ,

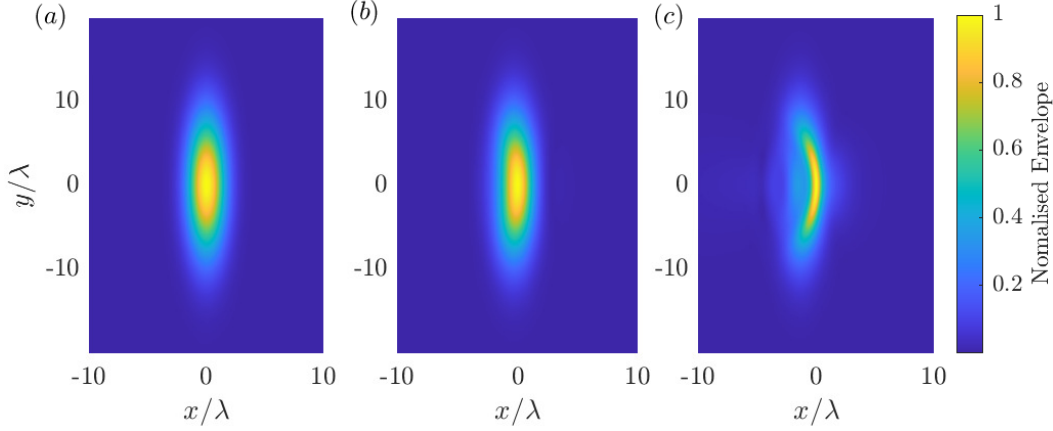


**FIGURE 4.** Averaged shape of NewWave groups (a): NewWave profile calculated based on the underlying wave spectrum with Quasi-determinism theory, (b,c): wave groups profile at nonlinear focus with initial conditions based on NewWave profile for top 100 largest events captured during the random simulations. Figure (b) presents results for the Case 1 in Table 2 and (c) presents results for the Case 3 Table 2. Envelope profile are normalised and centred by the maximum value at the envelope peak.

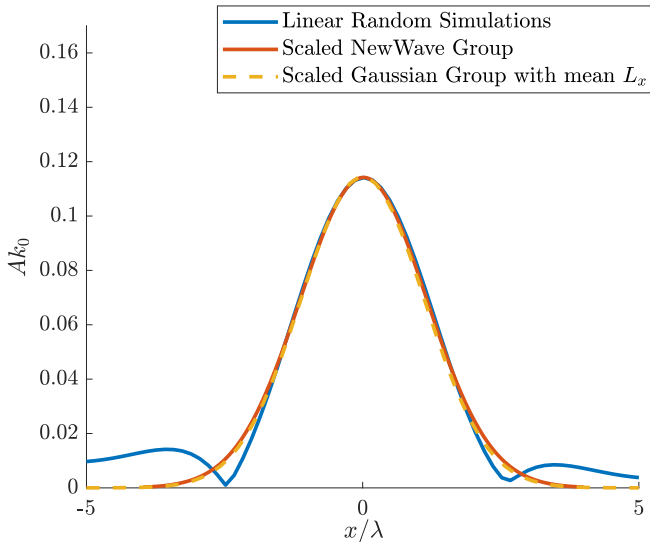


**FIGURE 5.** Average shape comparison in the mean wave direction for Case 1 in Table 2. The blue line shows the averaged shape of Top 3 largest events from linear simulation of random wave fields. The red line shows the NewWave profile, and the yellow line shows the Gaussian Wave group profile shown in Equation 2 with  $L_x$  value set to the averaged value of all decomposed large wave groups. Red and yellow lines are scaled to a peak value of the blue line for comparison purposes.

where  $A_{nonlinear}$  is the maximum envelope amplitude during the nonlinear evolution). The contraction of the envelope in the mean wave direction can also be quantified as the change in the envelope width at 80% of maximum envelope height (see

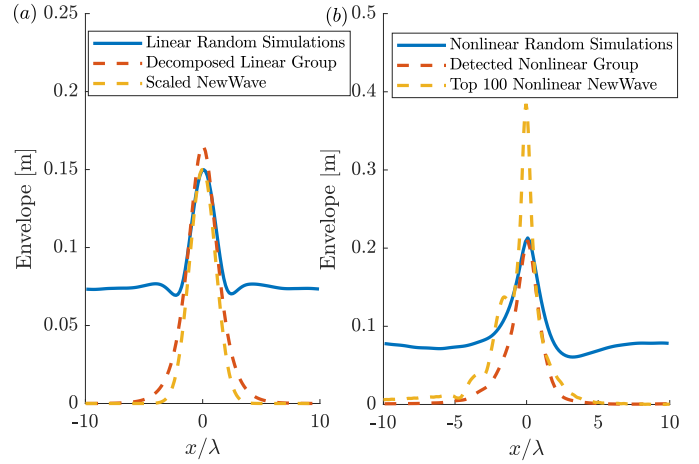


**FIGURE 6.** Average shape comparison in the mean wave direction for Case 3 in Table 2, (a): linear envelope profiles from random simulations in Figure 2 b (blue line), averaged decomposed linear wave group profile in Figure 3 b (red line), and NewWave profile Figure 4 a (yellow line), (b): nonlinear wave group profiles from random simulations in Figure 2 d (blue line), averaged decomposed wave group profile in Figure 3 d (red line), and wave groups profile at nonlinear focus with initial conditions based on NewWave profile for top 100 largest events captured during the random simulations in Figure 4 c (yellow line).

also [18]). In Figure 7, we present the comparison between the predictions based on the wave group detection method and the actual measured envelope profile in the nonlinear random wave fields. The envelope width decreases significantly as the local wave steepness increases, which agrees well with previous stud-

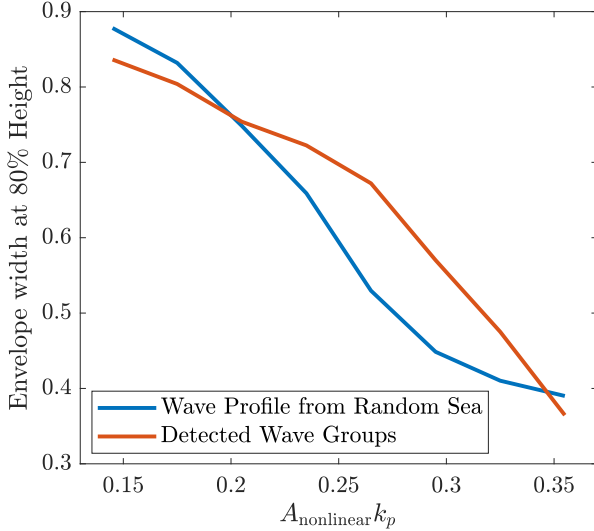


**FIGURE 7.** Envelope width in the mean wave direction at 80% of maximum envelope height for wave groups with different local steepnesses at nonlinear focus. Envelope width is nondimensionalised with the peak wavelength.

ies [12, 18, 30]. Additionally, the wave group detection method can make quite accurate predictions over a wide range of local wave steepness, which suggests such a method can be applied to a reasonable range of sea states and still maintain its accuracy in predictions.

## 5 Discussions and conclusions

In this study, we explore the nonlinear changes in the averaged shape of the largest events from random simulations of directionally spread seas. Additionally, we also explore whether it is possible to make predictions of these nonlinear changes in the random wave fields with deterministic wave groups. The initial conditions of these deterministic wave groups can either be obtained from the wave group detection algorithm proposed in previous studies [1, 2], or can be calculated from Quasi-determinism theory based on the underlying spectrum. We consider three cases with sampling domain sizes varying from an Eulerian point measurement to space-time measurement over an area. We find that nonlinear physics modifies the averaged shape of the largest events in random simulations so that the wave group tends to contract in the mean wave direction and the envelope peak tends to move to the front of the wave group. These nonlinear changes are well qualitatively predicted by the nonlinear evolution of deterministic wave groups with both wave group detection algorithm and the Quasi-determinism theory. This also agrees well with previous findings [11, 12, 18]. This suggests a strong connection between the deterministic wave groups and those largest events that occur in the random wave field. These carefully designed

wave groups are likely capturing essentially very similar nonlinear physics, which affects the evolution of these rogue waves in the random wave fields.

Since it is likely that similar nonlinear physics is driving the nonlinear evolution for both the largest waves in the random wave field and the carefully designed wave groups, we further explore whether it is possible to make quantitative predictions on these nonlinear changes in the random wave fields with only deterministic wave groups. We present the predictions for the most nonlinear case with waves sampled over an area (i.e. Case 3). The quantitative comparison shows that the wave group with initial conditions determined by the wave group detection algorithm can make accurate predictions on both the nonlinear amplification as well as the nonlinear changes of the shape.

We note that care must be taken when using such data driven methods. Firstly, this data centric method has only been applied to numerical simulations based on MNLS. Data pre-processing may be required to remove noise before applying it to field observations or experimental data. Additionally, due to the limitation on the computational resources, we only present one sea state in this study. However, based on the fact that the envelope contraction can be well captured with the wave group detection algorithm for a wide range of local steepness. We are confident that this method can make accurate predictions for a wide range of sea states.

Finally, we discuss the takeaway message from this study. In this study, we show that there are some connections between the averaged shape of the largest events from random wave fields and the carefully designed wave groups. These connections are likely due to both processes sharing similar underlying nonlinear physics and these two processes can be statistically linked via appropriate data driven methods. The wave group detection method proposed in [1] shows its edge in predicting these nonlinear changes in random wave fields with only wave groups. The advantage of using deterministic wave groups predicting nonlinear behaviour in random wave fields does not only limited to the computational savings and reduction in the experimental cost. The proposed data driven method also allows more localised nonlinear physics to be included for better predictions. For example, wave breaking in random wave fields can happen randomly in time and space, which is almost impractical to trace and explore in detail. However, wave groups with predefined phases and amplitudes are much easier to investigate. Hence, we do believe such a method connecting the individual wave groups with random wave fields does have a huge potential in ocean engineering practice.

## Acknowledgements

We thank Prof Paul Taylor (UWA) for his input into aspects of this work. This work was supported by the EPSRC grant number EP/V050079/1.

## REFERENCES

- [1] Tang, T., and Adcock, T. A. A., 2022. “A reduced order model for space-time wave statistics using probabilistic decomposition-synthesis method”. *submitted, Ocean Eng.*
- [2] Farazmand, M., and Sapsis, T. P., 2017. “Reduced-order prediction of rogue waves in two-dimensional deep-water waves”. *J. Comput. Phys.*, **340**, pp. 418–434.
- [3] Kharif, C., and Pelinovsky, E., 2003. “Physical mechanisms of the rogue wave phenomenon”. *Eur. J. Mech.*, **22**(6), pp. 603–634.
- [4] Dysthe, K. B., Krogstad, H. E., and Müller, P., 2008. “Oceanic rogue waves”. *Annu. Rev. Fluid Mech.*, **40**(1), pp. 287–310.
- [5] Adcock, T. A. A., and Taylor, P. H., 2014. “The physics of anomalous (‘rogue’) ocean waves”. *Reports Prog. Phys.*, **77**(10), p. 105901.
- [6] Lindgren, G., 1970. “Some Properties of a Normal Process Near a Local Maximum”. *Ann. Math. Stat.*, **41**(6), pp. 1870–1883.
- [7] Boccotti, P., 1983. “Some new results on statistical properties of wind waves”. *Appl. Ocean Res.*, **5**(3), pp. 134–140.
- [8] Tromans, P. S., Anatrak, A. R., and Hagemeyer, P., 1991. “New model for the kinematics of large ocean waves application as a design wave”. *Proc. First Int. Offshore Polar Eng. Conf.*, **8**, pp. 64–71.
- [9] Fedele, F., and Tayfun, M. A., 2009. “On nonlinear wave groups and crest statistics”. *J. Fluid Mech.*, **620**, p. 221.
- [10] Gibbs, R. H., and Taylor, P. H., 2005. “Formation of walls of water in ‘fully’ nonlinear simulations”. *Appl. Ocean Res.*, **27**(3), jun, pp. 142–157.
- [11] Adcock, T. A. A., Gibbs, R. H., and Taylor, P. H., 2012. “The nonlinear evolution and approximate scaling of directionally spread wave groups on deep water”. *Proc. R. Soc. A Math. Phys. Eng. Sci.*, **468**(2145), pp. 2704–2721.
- [12] Adcock, T. A. A., Taylor, P. H., and Draper, S., 2015. “Nonlinear dynamics of wave-groups in random seas: unexpected walls of water in the open ocean”. *Proc. R. Soc. A Math. Phys. Eng. Sci.*, **471**(2184), dec.
- [13] Tang, T., Xu, W., Barratt, D., Bingham, H. B., Li, Y., Taylor, P. H., van den Bremer, T. S., and Adcock, T. A. A., 2020. “Spatial evolution of the kurtosis of steep unidirectional random waves”. *J. Fluid Mech.*, **908**.
- [14] Tang, T., and Adcock, T. A. A., 2021. “The influence of finite depth on the evolution of extreme wave statistics in numerical wave tanks”. *Coast. Eng.*, **166**, p. 103870.
- [15] Latheef, M., Swan, C., and Spinneken, J., 2017. “A laboratory study of nonlinear changes in the directionality of extreme seas”. *Proc. R. Soc. A Math. Phys. Eng. Sci.*, **473**(2199), p. 20160290.
- [16] Karpadakis, I., Swan, C., and Christou, M., 2019. “Laboratory investigation of crest height statistics in intermediate water depths”. *Proc. R. Soc. A Math. Phys. Eng. Sci.*, **475**(2229), p. 20190183.
- [17] Gemmrich, J., and Thomson, J., 2017. “Observations of the shape and group dynamics of rogue waves”. *Geophys. Res. Lett.*, **44**(4), feb, pp. 1823–1830.
- [18] Tang, T., Tromans, P. S., and Adcock, T. A. A., 2019. “Field measurement of nonlinear changes to large gravity wave groups”. *J. Fluid Mech.*, **873**, pp. 1158–1178.
- [19] Mohamad, M. A., Cousins, W., and Sapsis, T. P., 2016. “A probabilistic decomposition synthesis method for the quantification of rare events due to internal instabilities”. *J. Comput. Phys.*, **322**, pp. 288–308.
- [20] Tang, T., and Adcock, T. A. A., 2022. “Estimating space-time wave statistics using a sequential sampling method and Gaussian process regression”. *Applied Ocean Research*, **122**, p. 103127.
- [21] Trulsen, K., Kliakhandler, I., Dysthe, K. B., and Velarde, M. G., 2000. “On weakly nonlinear modulation of waves on deep water”. *Phys. Fluids*, **12**(10), pp. 2432–2437.
- [22] Adcock, T. A. A., and Taylor, P. H., 2016. “Fast and local non-linear evolution of steep wave-groups on deep water: A comparison of approximate models to fully non-linear simulations”. *Phys. Fluids*, **28**(1), jan, p. 16601.
- [23] Barratt, D., van den Bremer, T. S., and Adcock, T. A. A., 2021. “MNLS simulations of surface wave groups with directional spreading in deep and finite depth waters”. *J. Ocean Eng. Mar. Energy*, pp. 1–15.
- [24] Dysthe, K. B., Trulsen, K., Krogstad, H. E., and Socquet-Juglard, H., 2003. “Evolution of a narrow-band spectrum of random surface gravity waves”. *J. Fluid Mech.*, **478**, pp. 1–10.
- [25] Lo, E., and Mei, C. C., 1985. “A numerical study of water-wave modulation based on a higher-order nonlinear Schrödinger equation”. *J. Fluid Mech.*, **150**, pp. 395–416.
- [26] Baldock, T. E., Swan, C., and Taylor, P. H., 1996. “A laboratory study of nonlinear surface waves on water”. *Philos. Trans. Royal Soc. A Math. Phys. Eng. Sci.*, **354**(1707), pp. 649–676.
- [27] Gibson, R. S., and Swan, C., 2006. “The evolution of large ocean waves: the role of local and rapid spectral changes”. *Proc. R. Soc. A Math. Phys. Eng. Sci.*, **463**(2077), pp. 21–48.
- [28] Boccotti, P., 2000. *Wave mechanics for ocean engineering*. Elsevier.
- [29] Barratt, D., Bingham, H. B., Taylor, P. H., Van Den Bremer, T. S., and Adcock, T. A. A., 2021. “Rapid spectral evolution of steep surface wave groups with directional spreading”. *J. Fluid Mech.*, **907**.
- [30] Gibbs, R. H., 2004. “Walls of water on the open ocean”. PhD thesis, University of Oxford.